energy&fuels

pubs.acs.org/EF

Article

Detailed Molecular Composition of Wood Pyrolysis Bio-Oils Revealed by HPLC-FT-ICR MS

Martha L. Chacón-Patiño,* Joseph W. Frye-Jones, Lissa C. Anderson, Winston K. Robbins, Germain Salvato Vallverdu, Álvaro J. Tello-Rodríguez, Wladimir Ruiz, German Gascon, Christopher P. Rüger, David C. Dayton, Pierre Giusti, Charlotte Mase, Caroline Barrère-Mangote, Carlos Afonso, Brice Bouyssiere, and Ryan P. Rodgers*

Cite This: *Energy Fuels* 2025, 39, 3575−3588

Read Online

ACCESS | Metrics & More | Article Recommendations | Supporting Information

ABSTRACT: The highly complex nature of wood pyrolysis bio-oils, which contain thousands of distinct molecular species with varying ionization efficiencies, poses a significant challenge for characterization by direct-infusion high-resolution mass spectrometry. This study presents a novel method combining high-performance liquid chromatography (HPLC) with 21 Tesla Fourier transform ion cyclotron resonance mass spectrometry (21T FT-ICR MS) for detailed molecular characterization of bio-oils within the scope of negative-ion ESI. The HPLC method is optimized to separate polyfunctional oxygen-containing molecules using a polymeric stationary phase with dimethylaminopropyl functionalities, and a methanol−water eluent with dimethylamine. The acidic compounds in bio-oils equilibrate between the DEA-containing mobile phase and the stationary phase, facilitating efficient gradient elution of oxygen-rich species. Coupling online HPLC with 21T FT-ICR MS revealed ∼3,000 additional monoisotopic O_x molecular formulas compared to direct-infusion FT-ICR MS. Newly detected compounds exhibited higher H/C ratios and a wider range of oxygen content, characteristic of low-molecular-weight carbohydrates and species with a composition that resembles biomass. The method enabled the detection of carbohydrate-like species (O/C ≈ 1, H/C ≈ 2) and highly aromatic compounds (H/C < 0.6, O/C < 0.3) that were undetectable via direct infusion. Early eluting, methanol-soluble species showed higher H/C ratios (∼1.5 to 2.0) and oxygen content consistent with lignin oligomers, while later-eluting compounds exhibited increased aromaticity, with compositions typical of condensed aromatic species. Advanced data processing using a Python-based, PyC2MC, software package further revealed compositional trends aligned with the solubility of bio-oils. Despite the overlap between LC−MS and direct infusion MS, single ion chromatograms revealed distinct elution patterns for identical molecular formulas, providing insights into potential isomeric diversity that are not accessible through direct infusion analyses. These findings demonstrate the enhanced molecular-level characterization achieved by HPLC-FT-ICR MS, providing key insights into the intricate composition of bio-oils and their potential for energy applications. The proposed approach provides a unique perspective on isomeric diversity and the distribution of functional groups, laying the groundwork for understanding the molecular basis of reactivity and upgrading potential in bio-oils. As the developed method targets the separation and characterization of polyfunctional oxygen-containing species, it can also be applied to dissolved/natural organic matter, photo-oxidation products, and emerging contaminants, e.g., water-soluble species leaching from materials like asphalt and petroleum-based road sealants.

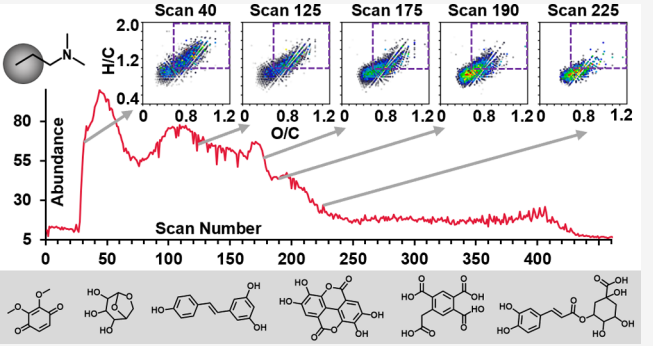

Downloaded via FLORIDA STATE UNIV on March 3, 2025 at 14:36:07 (UTC).
See https://pubs.acs.org/sharingguidelines for options on how to legitimately share published articles.

1. INTRODUCTION

Advanced biofuels, produced by hydrotreating bio-oil intermediates from fast pyrolysis of nonfood biomass, can be integrated into a sustainable carbon cycle, where the carbon released during combustion is reabsorbed during biomass growth, offering a pathway to net-zero carbon emissions in the transportation sector.[1] This short-term, closed-loop system ensures that the total amount of atmospheric CO_2 remains nearly balanced, unlike the consumption of fossil fuels, which introduces carbon sequestered for millions of years into the environment.[2]

Received: November 19, 2024
Revised: January 9, 2025
Accepted: January 14, 2025
Published: February 7, 2025

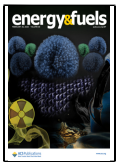

© 2025 American Chemical Society

https://doi.org/10.1021/acs.energyfuels.4c05674
Energy Fuels 2025, 39, 3575−3588

There are numerous pyrolysis technologies for converting biomass into liquid bio-oil intermediates.[3−5] The primary goal of these technologies is to maximize both the yield and the quality of bio-oil for high-carbon-efficiency biofuel production. While the definition of yield is straightforward, bio-oil quality is more nuanced and relates to how effectively these intermediates can be upgraded into fuels and chemicals. The simplest measure of bio-oil quality is bulk oxygen content, which is typically determined by elemental analysis.[6] Unfortunately, bulk oxygen content only provides an empirical correlation and offers little predictive power in assessing how the elemental composition of different bio-oils will impact upgrading performance.[7,8]

Bio-oils are highly complex mixtures with extremely diverse chemical functionalities, broad boiling point ranges, and wide molecular weight distributions. They are primarily generated through the thermal decomposition of cellulose, hemicellulose, and lignin, resulting in molecular characteristics inherited from these biopolymers. During pyrolysis, cellulose degrades into pyrans, furans, and oxygenated compounds such as levoglucosan, 5-hydroxymethylfurfural, and furfural, alongside low-molecular-weight aldehydes like acetaldehyde.[9] Hemicellulose breaks down into anhydrosugars and small organic acids, while lignin fragments into phenols, alcohols, and aromatic hydrocarbons.[10] Secondary reactions between these primary decomposition products further increase the molecular diversity of bio-oils, ultimately leading to the formation of carbon-rich solids known as "char".

The inherent complexity of bio-oils poses a significant challenge for comprehensive chemical characterization, which is crucial to optimize refining and separation processes and identify opportunities to produce high-value chemicals, such as acetic acid.[11] Over the years, a wide variety of analytical methods have been applied to bio-oil analysis, addressing bulk, functional, and molecular-level characterization. At the bulk level, standard ASTM methods have been developed to determine elemental composition (CHONS), water content (via Karl Fischer titration), and Total Acid Number (TAN).[12] Gel permeation chromatography is also used at this level to determine molecular weight distributions.[13] For functional characterization, nuclear magnetic resonance (e.g., ^{31}P NMR)[14] identifies specific functional groups (e.g., hydroxyl). Finally, at the molecular level, gas chromatography with mass spectrometry (GCMS) or flame ionization detection (GC-FID) is used to identify volatile species.[15,16] In practice, the constraints of individual methods often necessitate employing a combination of analytical techniques to achieve a thorough chemical speciation. No single method can comprehensively characterize a whole bio-oil sample effectively.

Quantitative chemical analyses of bio-oils are typically performed using one- or two-dimensional GCMS, enabling the identification of several hundred compounds with high confidence and facilitating relative abundance comparisons across samples.[17,18] Semiquantitative methods often integrate chromatographic peak areas to estimate the relative abundance of individual compounds or groups of compounds. These areas, proportional to analyte concentrations, are typically grouped based on chemical functionality to simplify the interpretation of bio-oil composition.[19] While calibration standard mixtures can provide accurate quantification of specific compounds, this approach becomes impractical for bio-oils due to their extensive molecular complexity. Furthermore, GCMS and GC × GCMS are limited to analyzing the volatile and semivolatile fractions of bio-oils, typically accounting for only 25−40 wt % of the sample.[20] These methods are less effective for thermally labile or nonvolatile species. When electron ionization (EI) is employed, the extensive fragmentation it produces often weakens or eliminates molecular ion peaks, restricting identification to compounds with matching fragmentation patterns in mass spectral libraries. Consequently, novel or highly fragmented bio-oil components often remain undetected, highlighting the need for complementary analytical techniques to fully characterize the complexity of bio-oils.[21]

Advances in analytical methods and instrumentation have led to the development of more comprehensive ways to measure the chemical composition of bio-oils. One such technique is FT-ICR MS, which can identify a wide range of bio-oil components with the high mass resolving power necessary to reveal molecular-level details. In modern MS analyses, multiple atmospheric pressure ionization techniques, such as electrospray ionization (ESI), atmospheric pressure photoionization (APPI), and atmospheric pressure chemical ionization (APCI), are often employed. ESI is particularly effective for polar compounds, APPI targets less polar aromatic species, and APCI captures both aliphatic and aromatic molecules. By integrating these complementary techniques, the molecular diversity of bio-oils can be more comprehensively characterized.

FT-ICR MS accurately determines the exact mass of thousands of mass spectral peaks, assigning each a unique molecular formula based on its mass accuracy.[22] These formulas enable the calculation of double bond equivalents (DBE), which represent the number of rings and double bonds to carbon, providing a measure of molecular aromaticity.[23] Additionally, molecular formulas are classified based on their heteroatom content. For example, compounds with varying combinations of carbon and hydrogen, but containing eight oxygen atoms, are categorized into the O_8 class. To date, most bio-oil characterization by FT-ICR MS has been based on direct-infusion methods, commonly referred to as "dilute-and-shoot" analyses.[24] For instance, Mase,[25] Ware,[26] and Palacio-Lozano et al.,[27] have reported molecular formulas with oxygen content ranging from O_1 to O_{15} classes by direct-infusion FT-ICR MS. In all cases, the characterization of oak bio-oils revealed an extended carbon number range that far exceeds the capabilities of GCMS. The application of a petroleomics approach in the analysis of a loblolly pine bio-oil and its hydroprocessed effluents as a function of run time via direct infusion FT-ICR MS analysis yielded an exceptional agreement between mass spectrometry and bulk elemental composition trends due to processing. However, the mass spectrometry results consistently overestimated the oxygen content and underestimated the hydrogen content of all samples. Thus, although the trend of the changes in O/C and H/C matched that of bulk elemental composition analysis, the overall precision was poor.[28]

FT-ICR MS analysis of bio-oils and their upgraded products has shown DBE values ranging from approximately 5−25, with carbon numbers between 10 and 50. In the case of "crude" bio-oils, a consistent increase in both DBE and carbon number is observed as the number of oxygen atoms per molecule increases, indicating the presence of oligomeric species.[29] Conversely, hydrotreated products display a narrower range of DBE and carbon number as oxygen content increases, suggesting direct deoxygenation. This observation is further supported by the fact that compound classes with high oxygen numbers (>O_7) retain their initial DBE values after hydrotreatment, ruling out hydrogenation pathways.[30]

https://doi.org/10.1021/acs.energyfuels.4c05674
Energy Fuels 2025, 39, 3575−3588

Molecular formulas can be visualized using van Krevelen diagrams, which plot H/C versus O/C ratios. For example, Palacio-Lozano et al. employed van Krevelen diagrams to track changes in H/C and O/C ratios during bio-oil upgrading, finding that these changes included the simultaneous loss of CO_2 and gain of H_2, which resulted in an increased concentration of bio-oil molecules suitable for fuel applications.[31] In a separate study, k-means clustering was applied to van Krevelen diagrams to assess the effects of accelerated aging on bio-oil fractions, revealing that aging led to increased DBE and oxygen content, indicating molecular condensation and oxidation.[32]

Although direct-infusion FT-ICR MS has been highly valuable for investigating the molecular composition of complex mixtures, this approach is limited by ion suppression and provides little-to-no information about chemical functionality and isomers. When multiple species compete for ionization, those with higher ionization efficiencies dominate the process, which reduces the likelihood of detecting compounds with lower abundance or ionization efficiencies.[33] Chromatographic separations can overcome this by reducing the coelution of analytes. Most studies on liquid chromatography applied to pyrolysis bio-oils focus on water-soluble components. For example, Lazzari et al. used comprehensive two-dimensional liquid chromatography (LC × LC) to analyze the aqueous phase of pyrolysis bio-oils derived from sources such as coconut fibers, pineapple leaves, and cassava peel.[34] By integrating two reversed-phase (RP) separations and coupling them with UV−vis and ESI-MS detection, the authors successfully identified and quantified 28 compounds, primarily phenols, ketones, and aldehydes. In another study, Crepier et al. employed supercritical fluid chromatography (SFC) using ethylpyridine-bonded silica gel as the stationary phase and acetonitrile−water as eluents.[35] The authors demonstrated the detection of approximately 120 chromatographic peaks in just 22 min.

In 2021, Rowland et al. coupled online liquid chromatography with 21T FT-ICR MS for analysis of petroleum.[36] High magnetic field strength was critical for handling large ion populations ($>1 \times 10^6$) to achieve a high dynamic range per (single-scan) MS spectrum while maintaining the mass resolving power required at chromatographic time scales. For bio-oils, the use of high-field FT-ICR MS is similarly crucial, as their complexity and high heteroatom content also demand ultrahigh resolving power and mass measurement accuracy. In this work, we introduce a novel HPLC method coupled with negative-ion electrospray ionization (−ESI)−21T FT-ICR MS to analyze the complex molecular composition of acidic polyfunctional oxygenates in wood pyrolysis bio-oils. This approach revealed over ∼3000 additional molecular formulas compared to direct-infusion MS, offering deeper insights into bio-oil compounds and elution patterns indicative of isomeric diversity, including lignin-derived oligomers and carbohydrate-like species. The results demonstrate the power of combining novel chromatographic separations with FT-ICR MS to achieve a more comprehensive and accurate profile of oxygen-containing species in wood pyrolysis bio-oils.

2. EXPERIMENTAL SECTION

2.1. Materials and Sample Description. High Performance Liquid Chromatography (HPLC) grade methanol (MeOH), tetrahydrofuran (THF), hexane, dichloromethane (DCM) and toluene (Tol), puriss. p.a. grade diethylamine (DEA) and model compounds were purchased from MilliporeSigma. Liquid chromatography−mass spectrometry grade water (H_2O) was supplied by Honeywell Research Chemicals. All solvents were used as received. The POROS stationary phase, featuring a dimethylaminopropyl functional group attached to a polymeric backbone, was selected for the HPLC separation of bio-oils. The amino functionalities of this material facilitate interactions with the acidic groups present in bio-oils. A 0.5 × 5.0 cm POROS column (GoPure D) was purchased from Thermo Fisher Scientific.

Pinewood pyrolysis bio-oil samples were supplied by BTG BTL Company (now BTG bioliquids, Enschede, Netherlands) and RTI International (North Carolina, United States). The BTG BTL bio-oil was produced by fast pyrolysis of pinewood. The RTI bio-oil was produced at a 1-ton-per-day pilot plant at a temperature of 464 °C and a 49.5 kg/h feed rate. The process utilized gamma alumina as a catalyst. The resulting bio-oil was fractionated by liquid−liquid extraction with toluene and water. An additional upgraded RTI bio-oil sample was produced by reactive catalytic fast pyrolysis of loblolly pine in a lab-scale fluidized bed reactor (2.5 in. diameter) under a hydrogen-rich atmosphere (80 vol %). The process used a MoO_3 catalyst on TiO_2 and ZrO_2 supports at a mean temperature of 500 °C, with a feed rate of 4−5 g per minute.

Two samples with distinct chemistries were selected to evaluate the HPLC separation: alkali-extracted lignin and the "F4 UASE" fraction. Alkali lignin (Kraft lignin) was purchased from MilliporeSigma and used as a lignin base. To solubilize the lignin, 200 mg was dispersed in 3 mL of THF, followed by the addition of 2 drops of concentrated HCl. The THF-solubilized, alkali lignin was then separated from the resulting solids, including alkaline chloride salts and any excess of unreacted lignin. While alkali lignin composition can vary based on preparation conditions, its inclusion as a reference material is supported by its similarity to polar bio-oil fractions in terms of elution behavior and solubility characteristics, as discussed by Ruiz et al.[37] The F4 UASE fraction was obtained using ultrasound-assisted solvent extraction (UASE), a method developed to fractionate bio-oils based on solubility.[37] Approximately 1 g of the upgraded RTI bio-oil was sequentially extracted using *n*-hexane, toluene, and dichloromethane (DCM). For each extraction, the bio-oil sample was dispersed in 5 mL of solvent, followed by 10 min of sonication at 35 kHz, and centrifugation at 1500 rpm for 5 min. This process was repeated ten times per solvent. The remaining insoluble material after DCM extraction was designated as the F4 fraction, known for its high polarity and strong tendency to aggregate.[37]

2.2. HPLC-MS. HPLC separations were performed using a Waters Alliance e2695 separation module and a Waters 2998 PDA detector. Bio-oil samples were dissolved in methanol at a concentration of 10 mg/mL, and 30 μL of the solution, equivalent to approximately 0.125 mg of bio-oil, was injected onto the column. The mobile phases consisted of solvent A (methanol), solvent B (water with 2 vol % DEA), and solvent C (water with 5 vol % DEA). The flow rate was maintained at 0.5 mL/min. The gradient started with 100% solvent A. After an initial hold for 8 min, solvent B was introduced at a rate of 2% per minute, reaching approximately 50% B at minute 25. Between minutes 25 and 28, the concentration of solvent B was rapidly increased at a rate of approximately 13.33% per minute to reach 90% B. Thus, the final steps of the elution program involved using a 1:9 ratio of A:B for 6 min, followed by a "wash" step with a 1:9 ratio of A:C to ensure complete elution of bio-oil species from the column. The column was reconditioned by ramping back down to 100% A for 10 min.

The effluent from the PDA detector was divided into two streams at a 50:1 ratio, with one stream going to waste and the other to a heated electrospray ionization (ESI) source for FT-ICR MS detection. All mass spectrometric data were collected using negative-ion electrospray ionization (−ESI) unless otherwise stated. The source was operated at 10 μL/min, with the probe temperature maintained at 40 °C and the ionization voltage set to −3.75 kV. The N_2 sheath gas and auxiliary gas were set at 15 (arbitrary flow units). Samples were directly ionized into the inlet of a custom-designed 21T FT-ICR mass spectrometer.[38] Approximately 2×10^6 charges were accumulated in a Velos Pro dual-cell linear ion trap (Thermo Fisher Scientific, maximum injection time of 1000 ms), transferred to an external multipole storage device, and

https://doi.org/10.1021/acs.energyfuels.4c05674
Energy Fuels 2025, 39, 3575−3588

ejected with an auxiliary RF[39] to a dynamically harmonized cell[40] operating at −6 V trapping potential.[41] Time-domain transients of 3.2 s (corresponding to 2.4×10^6 resolving power at m/z 200) were collected over an m/z range of 180−2000 using Predator Acquisition data station.[42] For HPLC-MS experiments, 450 transients were collected per run. For direct infusion experiments, 50 μg/mL sample solutions were directly infused at 5 μL/min into the ESI ion source. FT-ICR data acquisition parameters matched those employed for HPLC-MS, and 150 transients were coadded for each sample.

2.3. Elution Trends for Model Compounds. Model compounds (described in Table S1) were analyzed using an Orbitrap Eclipse Tribrid (Thermo Fisher Scientific) mass spectrometer via direct infusion and HPLC. Initially, the model compounds were diluted in methanol to a concentration of 10 μM to evaluate their ionization behavior by direct infusion at a flow rate of 5.5 μL/min. For the HPLC experiments, the model compound solutions were mixed to a final concentration of 500 μM, eluted, and ionized under the same conditions as the bio-oil samples. The Orbitrap Eclipse was selected for model compound analysis due to the lower complexity of these mixtures, which contained no more than 15−20 molecular species. The resolving power and mass accuracy of the Orbitrap Eclipse were sufficient for these samples, and its high scan speed and efficiency allowed for rapid determination of ionization efficiencies and required concentrations.

2.4. Data Analysis. For FT-ICR data, Fourier transformation, phase correction, internal calibration, molecular formula assignments, and data visualization were done using custom Predator, PetroOrg©, and PyC2MC software.[43] Peak picking was performed at 6σ of the baseline noise. For LC data processing, peak detection, and comparison to direct infusion results, assigned elemental compositions were counted only once, irrespective of their retention time. For model compounds, data analysis was performed manually using Xcalibur software (Thermo Fisher Scientific). Molecular formula assignment was performed with the following boundaries: carbon (5−120), hydrogen (H/C ratio = 0.2−2.2), oxygen (O/C ratio = 0.0−1.2), nitrogen (0−4), sulfur (0−2), and boron (0−1, including isotopes ^{10}B and ^{11}B). Mass spectrometry data, including raw Predator data files, Thermo.raw files, peak lists, calibrated files, and Excel files containing assigned molecular formulas, are publicly available at the OSF, Open Science Framework, repository, DOI 10.17605/OSF.IO/E723N.

3. RESULTS AND DISCUSSION

Figure 1a shows the broadband mass spectrum of BTG BTL bio-oil, obtained by coaddition of 150 scans collected via direct infusion negative-ion ESI 21T FT-ICR MS. The spectrum contains over 11,000 detected peaks, with a 30 mDa mass window at m/z 591 displaying 30 distinct peaks and a baseline resolved 2.5 mDa mass-split, crucial for assigning molecular formulas to species with differing sulfur and oxygen content. Nearly 9,500 molecular formulas were assigned with an RMS error of 60 ppb, representing 95% of the total ion abundance. The results presented here are influenced by the ionization method used. Negative-ion electrospray ionization (ESI) is particularly suited for detecting acidic compounds, which are abundant in oxygen-rich, minimally refined pyrolysis bio-oils and ionize efficiently under these conditions. While this approach provides detailed molecular insights into acidic oxygen-containing species, incorporating complementary ionization methods, such as atmospheric pressure chemical ionization (APCI) or atmospheric pressure photoionization (APPI), would be necessary to capture less polar and nonacidic compounds, enabling a more complete characterization of bio-oil composition.

The assigned molecular formulas were grouped into compound classes based on their heteroatom content.[44] For example, species containing carbon, hydrogen, and ten oxygen atoms are classified into the O_{10} class. For clarity, this study

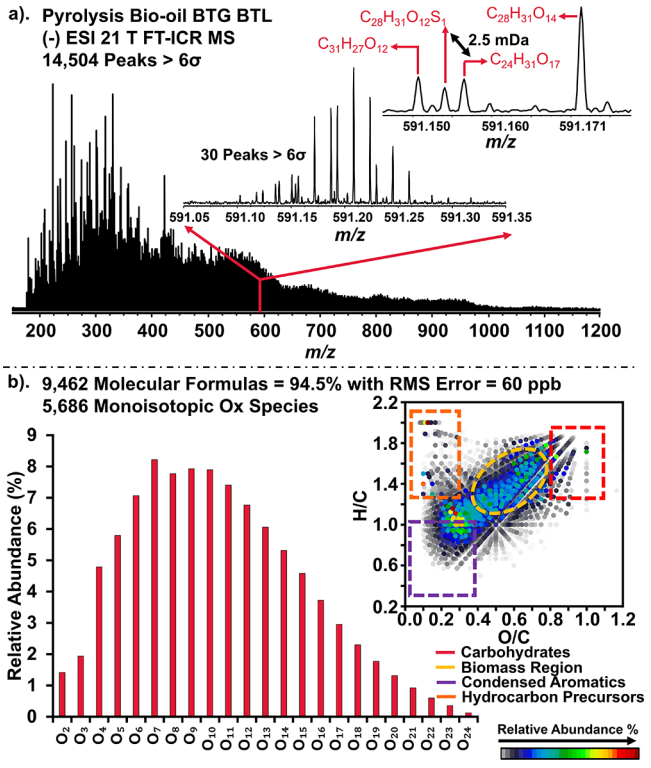

Figure 1. (a) Broadband mass spectrum of BTG BTL bio-oil obtained by direct infusion negative-ion ESI 21T FT-ICR MS, with zoom mass-insets at m/z 591. (b) Class distribution and van Krevelen diagram for monoisotopic O_x molecular formulas, highlighting the compositional range of compound families. Each region in the van Krevelen diagram represents a compound family based on H/C and O/C ratios: carbohydrates (high O/C ∼ 1, H/C ∼ 2), "biomass" species (0.4 < O/C < 0.8, 1.2 < H/C < 1.8), condensed aromatic species (low O/C < 0.4, H/C < 1), and hydrocarbon precursors (low oxygen, high H/C).

focuses on monoisotopic oxygen-containing compounds (O_1, O_2, O_3, etc.). Figure 1b highlights the identification of approximately 5,700 monoisotopic oxygen-containing species, covering a broad range of oxygen content, as shown in the class distribution bar graph. Molecules with up to 24 oxygen atoms were detected, suggesting the presence of multiple functional groups.

The compositional complexity of pyrolysis bio-oils is effectively visualized with van Krevelen diagrams. Each molecular formula is plotted as a dot according to its H/C and O/C ratios, with the color scale indicating its relative abundance. Distinct compound families are clustered in specific regions of the diagram.[45] For instance, biomass-related species, such as lignin and cellulose, appear in the range of 0.4 < O/C < 0.8 and 1.2 < H/C < 1.8, as shown in yellow in Figure 1b. Carbohydrates, which have significantly higher H/C ratios, often approaching 2.0, and O/C ratios near 1, occupy the red-highlighted region. In contrast, highly aromatic species are characterized by H/C ratios below 1. Molecules ideal for energy applications contain significantly more hydrogen and less oxygen, as indicated by the orange-highlighted region.[46] Van Krevelen diagrams are particularly useful for tracking compositional changes in bio-oils through catalytic conversion processes. For example, species initially located in the carbohydrate or biomass regions can be shifted toward the "highly-aromatic" compositional range following extensive dehydration. Advanced catalytic hydrogenation, with loss of CO and CO_2, coupled with

https://doi.org/10.1021/acs.energyfuels.4c05674
Energy Fuels 2025, 39, 3575−3588

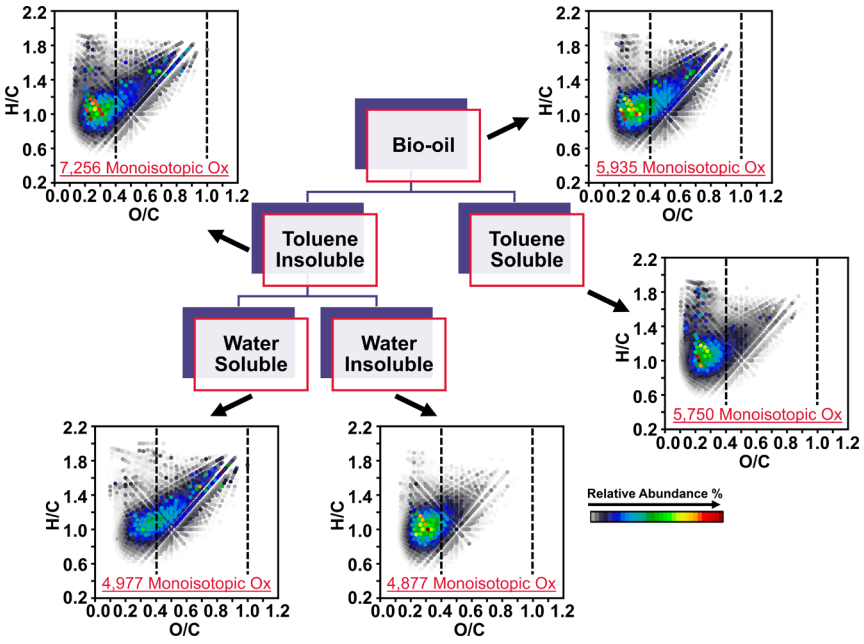

Figure 2. Van Krevelen diagrams of RTI loblolly pine pyrolysis bio-oil and its solubility fractions. Data were obtained by direct infusion negative-ion ESI 21T FT-ICR MS. Diagrams include only monoisotopic O_x molecular formula assignments. Black dashed lines indicate the O/C range of biomass and carbohydrates. Black dashed lines at O/C ratios of 0.4 and 1.0 provide visual reference points for comparing oxygen content across van Krevelen diagrams of the bio-oil sample and its fractions.

hydrogen uptake, shifts these highly aromatic molecules toward the ideal compositional range for energy applications. Furthermore, analogies to van Krevelen plots used in petroleum geochemistry could provide additional insights into bio-oil composition. Similar to the classification of source organic matter types and their maturity evolution in petroleum systems, these plots could be used to connect biomass feedstock types and pyrolysis conditions, such as temperature and heating time, to the resulting compositional trends in bio-oils.

The concept of molecular management is crucial in optimizing pyrolysis bio-oils for energy applications.[47] By applying advanced fractionation techniques, such as molecular distillation or liquid−liquid extractions, bio-oils can be separated into chemically distinct fractions that facilitate targeted upgrading. This selective processing allows for the enhancement of specific fuel properties, such as energy density and stability, while minimizing undesirable components like oxygenates.[48] Catalytic deoxygenation, for example, significantly increases the energy content of bio-oils, making them more compatible with existing petroleum refineries and suitable for transportation fuels.[49] Therefore, integrating molecular management strategies is essential to unlocking the full potential of bio-oils as a sustainable alternative to fossil fuels. Here, we employed a fractionation strategy that divided the bio-oil into toluene-soluble and toluene-insoluble fractions. The toluene-insoluble fraction was further separated based on solubility in water into water-soluble and water-insoluble fractions.

Figure 2 presents van Krevelen diagrams for the RTI bio-oil sample derived from loblolly pine pyrolysis and its corresponding solubility fractions. The data were obtained via direct infusion negative-ion ESI 21T FT-ICR MS. The whole bio-oil sample exhibits a molecular composition typical of pyrolysis bio-oils, with a wide range of oxygen content and abundant species having O/C ratios from 0.1 to 1.0. The black dashed lines highlight the O/C range of biomass and carbohydrates, indicating that the "parent" or unfractionated bio-oil is rich in these compositions, as well as in oxygen-depleted molecules (O/C < 0.4) with high aromaticity or low H/C ratios (<1.1). In the fractionated samples, the toluene-soluble portion contains fewer carbohydrate and biomass species, which appear more concentrated in the toluene-insoluble fraction. The water-soluble fraction features a high abundance of molecules in the biomass/carbohydrate region, while the water-insoluble fraction is highly aromatic, residing predominantly in the compositional range of soluble organic species, which has been reported for extracted organics from biochar.[50] The parent bio-oil sample revealed approximately 5,900 monoisotopic O_x molecular formulas, whereas the combined fractions (toluene-soluble, water-soluble, and water-insoluble) yielded around 9,000 unique monoisotopic O_x species. These results highlight the critical role of chemical separations in providing a more comprehensive understanding of bio-oil composition.

The fractionation scheme shown in Figure 2 was designed to separate bio-oil into chemically distinct fractions based on solubility differences, facilitating targeted molecular characterization. Toluene was selected as the primary solvent for this fractionation due to its aromatic, nonpolar nature, which effectively dissolves hydrophobic compounds, such as lignin-derived oligomers and polycyclic aromatic hydrocarbons (PAHs). Despite the nonpolar nature of toluene, the use of negative-ion ESI enables the detection of oxygen-enriched species within the toluene-soluble fraction, providing complementary insights into its composition. This approach ensures a more extended characterization of bio-oil fractions by leveraging the solubility properties of toluene to isolate specific classes of compounds while utilizing the sensitivity of negative-ion ESI for polar species.

Despite their markedly different solubility, the water-insoluble and toluene-soluble fractions display a nearly identical compositional range. This observation points to potential issues caused by ion suppression during direct infusion ESI-MS analysis. Given the thousands of molecular species with a wide range of

https://doi.org/10.1021/acs.energyfuels.4c05674
Energy Fuels 2025, 39, 3575−3588

ionization efficiencies, only a limited portion of these components is likely detected during MS characterization.[51] This prompted the development of a novel online HPLC separation, coupled with FT-ICR MS detection, to enhance molecular-level characterization. The method was initially developed for the fractionation of dissolved organic matter (DOM), drawing inspiration from the work of Rowland et al.,[52] which used aminopropyl silica (APS) gel SPE cartridges to fractionate naphthenic acids in fossil fuels. In that separation, carboxylic acids are adsorbed on the stationary phase through acid−base interactions, and fractions are eluted using methanol doped with formic acid, followed by the gradual introduction of dichloromethane.[53] As a result, the later-eluting fractions are enriched with more hydrophobic species.

Applying the same APS method to bio-oil separation resulted in more than 50% of the material irreversibly adsorbed onto the stationary phase. Polyfunctional oxygen-containing species, such as those found in DOM and bio-oils, are more effectively desorbed from amino functionalities at high pH.[54] In subsequent attempts to separate bio-oil samples using APS cartridges, the elution began with 100% methanol, followed by a gradual transition to pH-10 water. While direct infusion FT-ICR MS analysis of the early eluting SPE fractions showed promising compositional trends, concerns arose over the mobilization of the silica gel at high pH.[55] To address this issue, a polymeric stationary phase, i.e., poly(styrene-*co*-divinylbenzene) copolymer with dimethylaminopropyl functionalities, was chosen as an alternative to aminopropyl silica gel. Methanol and water were selected as eluents, but instead of using ammonium hydroxide to adjust the pH, DEA was added to the water, acting as a mobile phase modifier and a displacement additive.[56] Figure 3a illustrates the HPLC gradient. The separation starts with 100% methanol, and after 8 min, the water content (containing 2% DEA) gradually increases, reaching 90% by 30 min.

3.1. Separation Mechanism and Role of DEA. The separation method employed in this study leverages the interaction between the acidic functionalities of the analytes and the basic (dimethylamine) groups of the stationary phase. In the absence of DEA, acidic analytes remain strongly bound to the stationary phase, whereas nonacidic and weakly acidic compounds, such as carbohydrates and phenolics, are readily eluted with methanol. We hypothesize that when DEA is introduced, the separation proceeds via partition chromatography. The acids equilibrate between the mobile phase (containing DEA) and the stationary phase. As the water content in the eluent increases, a secondary separation occurs based on the hydrophilicity of the molecules. Compounds with more hydroxyl groups (higher O/C ratios) are retained longer due to stronger hydrogen bonding interactions with the stationary phase and are gradually eluted as the water (with 2% DEA) concentration rises. Therefore, to ensure complete elution, an additional 8 min "washing" step is performed at the end of the separation with 90% water containing 5% DEA. Previous studies demonstrated that DEA was used to overcome inconsistencies in cyano and amino columns by passivating unreacted silanol sites, which would otherwise act as acids and retain basic compounds.[54] In our case, however, DEA primarily facilitates partition chromatography without significant ionization or pH effects, as the 2% DEA solution has a pH greater than 10.[57−59]

3.2. Model Compounds. The separation method was evaluated using model compounds that could hypothetically resemble the species present in bio-oil samples. Figure 3b

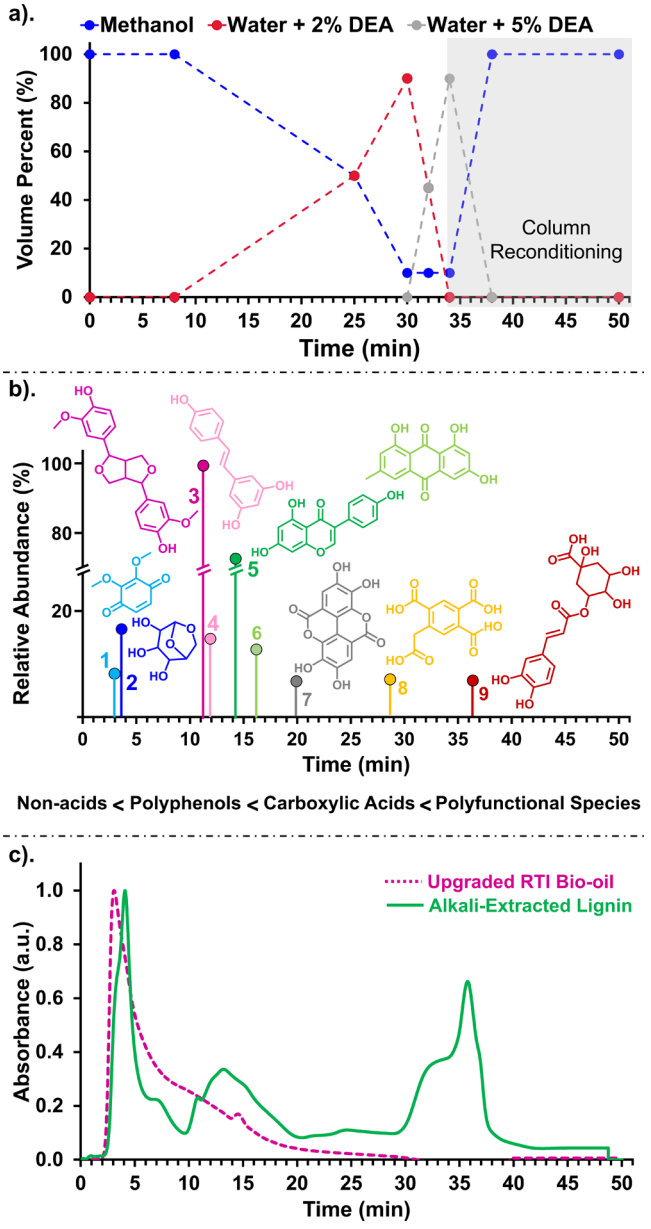

Figure 3. (a) HPLC gradient used for characterization of wood pyrolysis bio-oils; (b) elution trends for nine representative model compounds, obtained using negative-ion ESI with MS detection on an Orbitrap Eclipse; (c) PDA chromatograms at 310 nm for the upgraded RTI bio-oil (pink) and alkali-extracted lignin (green). UV−vis spectra are blank-subtracted and normalized.

summarizes the elution trends of nine model compounds, including levoglucosan, polyphenols like resveratrol, two isomers (in green), a tetracarboxylic acid (in yellow), and a polyfunctional compound containing phenol, hydroxyl, and carboxylic acid groups (in red). The data are represented by the centroids of the chromatographic peaks. Compounds 1 and 2, which lack acidic functionalities, did not bind to the column and were eluted with 100% methanol. For polyphenols 3 and 4, the presence of additional oxygen atoms, particularly in phenol functionalities, led to stronger interactions with the stationary phase. In the case of isomers 5 and 6, increased electron conjugation translated into greater acidity, resulting in longer retention times. Comparatively, the tetracarboxylic acid (compound 8) exhibited greater retention than the highly

https://doi.org/10.1021/acs.energyfuels.4c05674
Energy Fuels 2025, 39, 3575−3588

aromatic polyphenol (compound 7), despite their similar oxygen content. Finally, the polyfunctional molecule eluted at the end of the separation, reflecting its complex interaction with the stationary phase.

The elution trends for the model compounds suggest the following retention order: nonacids < polyphenols < carboxylic acids < polyfunctional species. Based on this, one would expect alkali-extracted lignin to contain a high concentration of polyphenols and polyfunctional species, causing it to elute predominantly toward the end of the separation. In contrast, a highly refined (upgraded) bio-oil, obtained through catalytic hydrogenation, a process aimed at reducing acidic functionalities, is expected to elute early due to its probable high concentration of nonacidic compounds. Figure 3c shows the PDA chromatograms for the upgraded RTI bio-oil and alkali-extracted lignin. The results clearly demonstrate that the lignin sample is rich in polyfunctional species, while the highly refined bio-oil is enriched with nonacidic compounds. The elution behavior of the alkali-extracted lignin sample should be consistent with that of the most polar bio-oil fractions, since lignin-derived species are significant contributors to these fractions. This hypothesis aligns with findings from Ruiz et al.,[37] where alkali lignin was shown to share solubility and molecular weight distribution trends with polar bio-oil fractions. The use of alkali lignin as a comparative tool highlights the compositional relationship between bio-oil fractions and lignin-derived species, offering valuable insights into the molecular diversity of bio-oil. As the elution behavior of model compounds, upgraded RTI bio-oil, and alkali-extracted lignin revealed distinct trends in hydrophilicity and functionality, we next examined the elution behavior of the whole "parent" bio-oil and its solubility fractions (discussed in Figure 2).

Figure 4 presents the PDA chromatograms for the non-fractionated parent bio-oil sample and its solubility fractions. A

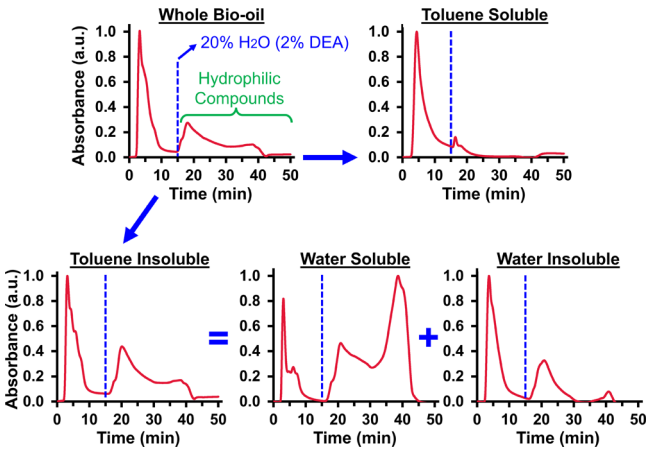

Figure 4. HPLC-PDA chromatograms at 310 nm for the parent pyrolysis bio-oil and its molecular-management fractions. Dashed blue line marks the point at 15 min where the eluent reaches 20% H_2O with 2% DEA, distinguishing between less hydrophilic and highly hydrophilic compounds. UV−vis spectra are blank-subtracted and normalized.

dashed blue line marks the point at which the eluent reaches 20% H_2O with 2% DEA, occurring at 15 min. Compounds eluting beyond this point are arbitrarily considered highly hydrophilic. The results indicate that the whole bio-oil sample contains compounds with a wide range of hydrophilicity, including a substantial portion of nonacidic species eluting with 100% methanol. Notably, ∼50% of the PDA signal is observed after 15 min of elution, indicating that approximately half of the sample consists of highly hydrophilic components. In contrast, the toluene-soluble fraction is less hydrophilic, with most of the PDA signal (∼85%) originating from species eluting before 15 min, as expected. The toluene insolubles are further fractionated into water-soluble and water-insoluble species. The water-soluble fraction primarily consists of highly hydrophilic components, with around ∼70% of the PDA signal occurring after 15 min. In contrast, the water-insoluble fraction displays a more balanced distribution between methanol-eluted and highly hydrophilic compounds. These results indicate that the distinct elution behavior of each fraction, consistent with their solubility, provides insights into the distribution of chemical functionalities in wood pyrolysis bio-oils, thereby enhancing our understanding of their molecular composition.

The HPLC effluent from the PDA detector was directed to the HESI source via a 1/50 splitter, allowing detection by 21T FT-ICR MS. Figure 5a shows the total ion chromatogram for the water-soluble bio-oil fraction. Gray dashed lines help visualize and correlate specific scan numbers with time and eluent composition. Approximately 450 scans were acquired per HPLC-MS experiment, with an average scan time of ∼6.5 s. Figure 5a also includes van Krevelen diagrams for selected scans, with abundance-weighted H/C ratios. Species highly soluble in methanol, identified in scans 53 and 80, exhibit a broad range of O/C and H/C ratios, aligning with characteristics of carbohydrates and compositions in the biomass region. As the separation progresses, scan 130, with an eluent composition of approximately 20% water, shows a significant presence of species in the biomass region. Scans 210 and 278 reveal a shift toward an intermediate compositional range between the biomass and "highly aromatic" regions, suggesting extended dehydration during pyrolysis. Toward the end of the elution, scans 344 and 380 show a high concentration of highly aromatic molecules with lower H/C and O/C ratios. This compositional range is consistent with extractable species from biochar.

Figure 5b demonstrates the performance of 21T FT-ICR MS in a single scan. The broadband mass spectrum for scan 64 is shown, along with zoom-insets at m/z 465 and m/z 665. At m/z 465, the peak with the highest signal-to-noise ratio (S/N ∼ 150) exhibits a resolving power of ∼1,000,000. Even at m/z 665, both the signal-to-noise ratio (S/N ∼ 27) and resolving power (RP ∼ 700,000) remain optimal for reliable molecular formula assignment. This scan, corresponding to an eluent composition of 100% methanol, contains around 5,000 peaks. Molecular formula assignment identified approximately 2,950 formulas, accounting for 95% of the detected ion abundance, with roughly 2,100 of them being monoisotopic O_x species.

The accuracy of the molecular attribution is visualized in the plot of error as a function of m/z. Remarkably, 95% of the compositions fall within an error tolerance of ±0.05 ppm, with a root-mean-square (RMS) error of less than 60 ppb. These results highlight the ability of 21T FT-ICR MS to capture the molecular complexity of bio-oils in a single scan. This capability allows for constructing van Krevelen diagrams comparable to those generated through direct infusion MS, which typically require the coaddition of over 100 scans. As shown in the van Krevelen diagram on the right of Figure 5b, the molecular formulas identified in scan 64 cover a broad range of oxygen content, with most species clustering in the biomass and

https://doi.org/10.1021/acs.energyfuels.4c05674
Energy Fuels 2025, 39, 3575−3588

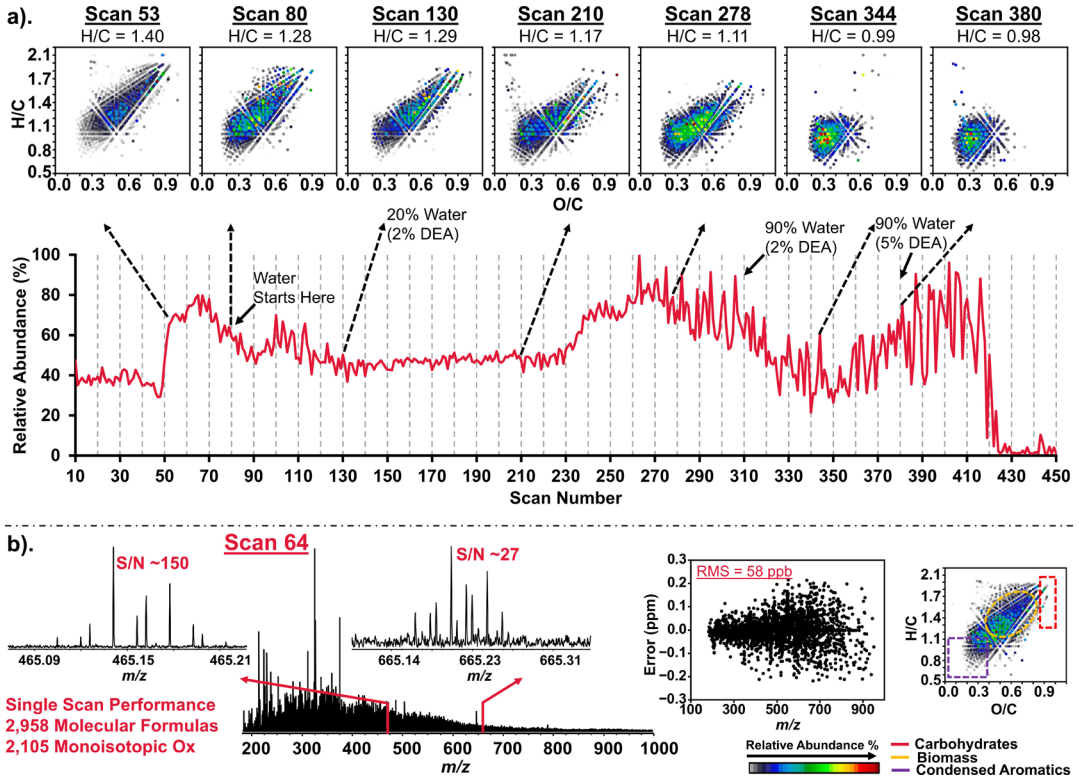

Figure 5. (a) Total ion chromatogram (TIC) of the water-soluble bio-oil fraction, showing ion abundance as a function of scan number. Van Krevelen diagrams and abundance-weighted H/C ratios illustrate the composition of selected scans. (b) Broadband mass spectrum and van Krevelen diagram for scan 64, with zoom insets at m/z 465 and m/z 665, demonstrating the ultrahigh resolving power and accurate molecular formula assignment achieved by —ESI 21T FT-ICR MS per single scan.

intermediate compositional regions, along with a notable abundance of carbohydrate-derived compounds.

Figure 6 presents the total ion chromatograms (TIC) obtained from HPLC-MS analysis of the water-soluble, water-insoluble, and toluene-soluble fractions of the RTI bio-oil sample. Each TIC is accompanied by a van Krevelen diagram that summarizes the combined, unique monoisotopic O_x molecular formulas detected from all scans, alongside the corresponding diagrams from direct infusion experiments (shown on the right). Dashed lines have been added to each pair of van Krevelen diagrams (HPLC-MS and direct infusion) to facilitate direct comparison between the compositional distributions of molecular formulas identified in each fraction. The number of detected monoisotopic O_x compositions is indicated in red for HPLC and purple for direct infusion. HPLC coupled with FT-ICR MS consistently reveals additional molecular composition information across all fractions compared to direct infusion. For example, for the water-soluble fraction, HPLC-MS analysis identified 7,704 species compared to 4,977 by direct infusion. This illustrates the ability of HPLC-MS to provide a more detailed molecular profile, especially in the carbohydrate and biomass regions, where molecular formulas with O/C = 1 are more prevalent. For the toluene-soluble fraction, LCMS more effectively identifies highly aromatic species, which are less accessible by direct infusion.

The TICs in Figure 6 should be interpreted alongside the PDA chromatograms from Figure 4, which reveal distinct differences in the distribution of functional groups throughout the chromatographic runs. For instance, the PDA chromatograms indicate that the toluene-soluble fraction elutes predominantly before the 15 min mark, suggesting a composition rich in nonacidic, less hydrophilic species. In contrast, the water-soluble and water-insoluble fractions feature stronger PDA signals in the highly hydrophilic region, pointing to the predominance of carboxylic acids and polyfunctional species. This comparison highlights the value of combining multiple detection modalities with HPLC to provide deeper insights into the functional group diversity of bio-oil fractions, insights that would not be as evident from TICs or direct infusion FT-ICR MS alone.

Having demonstrated the superior molecular characterization provided by HPLC-MS, we applied the method to a particularly challenging sample: the F4 UASE fraction from the upgraded RTI bio-oil. This fraction, characterized by high polarity and a strong tendency to aggregate, presents difficulties in molecular analysis.[60] The fractionation was performed using ultrasound-assisted solvent extraction (UASE), a method designed to separate bio-oils based on solubility in solvents of increasing polarity. Figure 7a shows van Krevelen diagrams for monoisotopic O_x species detected by direct infusion (left) and HPLC-MS (right). HPLC-MS identified 7,531 monoisotopic O_x species, compared to 6,160 detected by direct infusion. The van Krevelen diagrams in Figure 7b focus on the unique species detected by each method, with HPLC-MS revealing 2,001 unique species, nearly three times the 637 unique species detected by direct infusion. This demonstrates the superior sensitivity of HPLC-MS in capturing a broader molecular composition.

Both HPLC-MS and direct infusion detect unique species, highlighting their complementary capabilities. HPLC-MS proves particularly effective in identifying compounds in the low O/C, low H/C region, associated with highly aromatic

https://doi.org/10.1021/acs.energyfuels.4c05674
Energy Fuels 2025, 39, 3575−3588

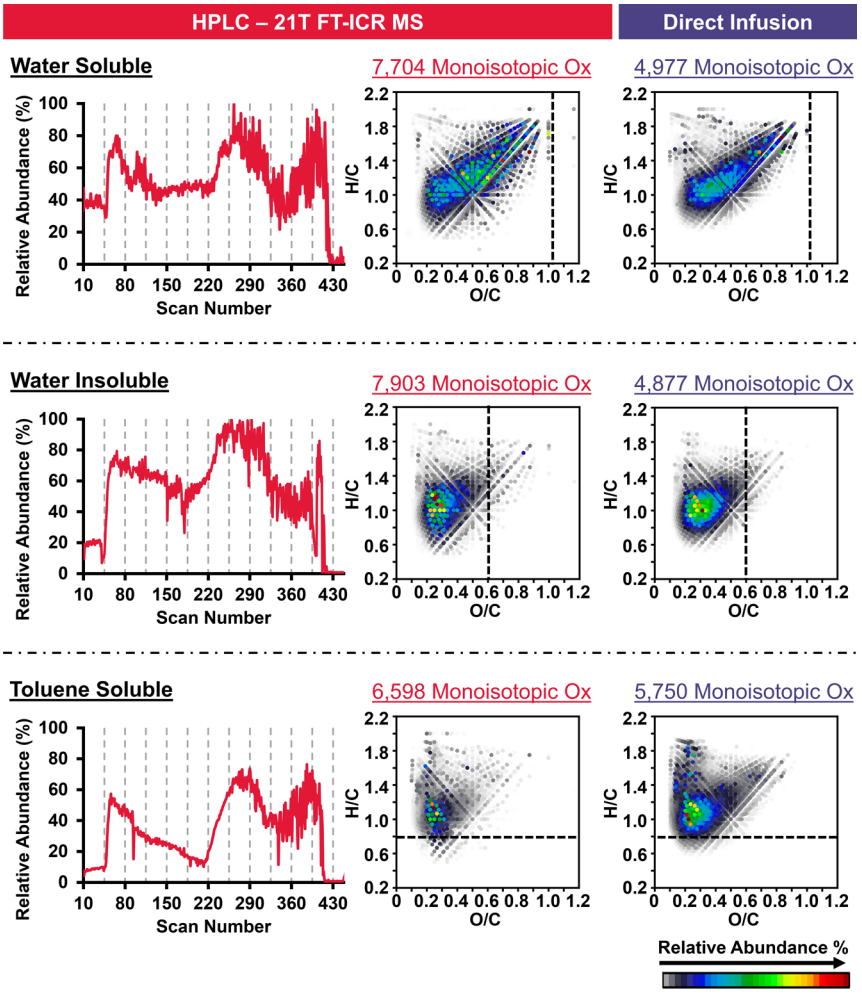

Figure 6. Total ion chromatograms (TIC) obtained via negative-ion ESI 21T FT-ICR MS for the water-soluble, water-insoluble, and toluene-soluble bio-oil fractions. Van Krevelen diagrams show unique, nonrepeated monoisotopic O_x molecular formulas from combined HPLC-MS scans (left) and direct infusion MS (right). Number of detected compositions is highlighted in red for HPLC-MS and purple for direct infusion MS. HPLC-MS reveals an extended number of molecular formulas and compositional trends across the fractions compared to direct infusion. Black dashed lines are included to facilitate visual comparison across van Krevelen diagram pairs for the different bio-oil fractions.

species missed by direct infusion. These aromatic, oxygen-deficient molecules are likely recalcitrant species formed during pyrolysis, with the potential to serve as coke precursors in catalytic upgrading due to their fouling tendencies.[61] In the carbohydrate region (H/C ≈ 2, O/C ≈ 1), HPLC-MS also showed substantial improvements, further highlighting its sensitivity to highly oxygenated species and a wide range of chemical functionalities. Overall, HPLC-MS captures a broader range of molecular species, offering deeper insights into the molecular complexity of highly polar fractions like F4 UASE. Combining HPLC-MS with direct infusion is essential for achieving a comprehensive understanding of pyrolysis bio-oils.

Figure 8a offers a more detailed examination of the F4 UASE fraction. The total ion chromatogram (TIC) reveals a complex elution profile, with analytes eluting across the entire chromatographic run, pointing to the chemical diversity of this highly polar fraction. Distinct oxygen classes are highlighted in "extracted mass spectra" from selected scans. For example, in scan 40, the extracted mass spectrum highlights peaks assigned to the O_7 and O_{10} classes. The red peaks correspond to molecular formulas in the O_7 class, with a prominent compound detected at m/z 205, identified as $[C_7H_{10}O_7{-}H]^-$. This compound is likely a carbohydrate derivative (as shown in Figure 8a, left), commonly formed during the pyrolysis of lignocellulosic material.[62] Similarly, the black peaks represent the O_{10} class, with the most abundant molecular formula, $C_{12}H_{20}O_{10}$ (neutral composition), consistent with cellobiosan, a recognized byproduct of wood pyrolysis.[63,64] In scan 50, the focus shifts to the O_8 class, where the dominant molecular formula, $C_{11}H_{18}O_8$, suggests an α-D-glucopyranoside derivative.[65] By scan 100, the O_8 class remains dominant, featuring molecular formulas that align with galactose acetate and a potential glucoside derivative.

Figure 8b depicts single ion chromatograms for selected molecular formulas. For example, the single ion chromatogram for the formula $C_7H_{10}O_7$ (H/C = 1.4, O/C = 1.0), likely a carbohydrate, shows that it elutes early in the chromatographic run, reflecting its lack of acidic functionalities. This behavior aligns with expectations, as nonacidic carbohydrates should have minimal interaction with the stationary phase, leading to early elution. The second single ion chromatogram, for the formula consistent with cellobiosan ($C_{12}H_{20}O_{10}$, O/C = 0.8), reveals a more complex elution pattern. Two distinct peaks are visible, suggesting the presence of isomers. The first region occurs early in the separation, consistent with weakly acidic species like cellobiosan, while the second elution peak indicates a possible

https://doi.org/10.1021/acs.energyfuels.4c05674
Energy Fuels 2025, 39, 3575−3588

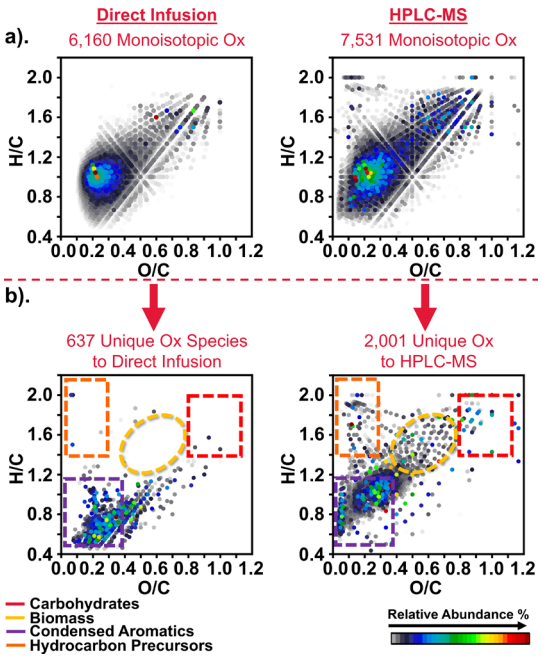

Figure 7. (a) Van Krevelen diagrams for monoisotopic O_x species detected in the F4 UASE fraction of upgraded RTI bio-oil by direct infusion (left) and HPLC-MS (right). (b) Van Krevelen diagrams highlighting the unique species detected by each method, with HPLC-MS revealing 2,001 unique species, nearly three times the 637 unique formulas detected by direct infusion. Color-coded regions represent different compound classes: red for carbohydrates, yellow for biomass, purple for highly aromatic species, and orange for hydrocarbon precursors. This demonstrates the superior sensitivity of HPLC-MS in capturing a broader molecular composition.

isomer with acidic functionalities, such as phenols. Lastly, the single ion chromatogram for $C_{22}H_{24}O_9$ (O/C = 0.4) shows even greater complexity in its elution profile, shifting toward the end of the chromatographic run. This behavior suggests the presence of multiple isomers, with the separation likely influenced by the polymeric component of the stationary phase, which has an aromatic nature. The poly(styrene-*co*-divinylbenzene) copolymer likely facilitates $\pi-\pi$ stacking interactions with aromatic species from the bio-oil, contributing to their extended retention.[66] Additionally, the amino functionalities on the stationary phase primarily support partition chromatography with acidic analytes. Thus, the delayed elution of molecules with lower O/C ratios and higher carbon content is likely due to a combination of partitioning behavior and $\pi-\pi$ stacking interactions, the latter being facilitated by the aromatic nature of the poly(styrene-*co*-divinylbenzene) copolymer, which selectively retains aromatic species from the bio-oil.

4. CONCLUSIONS

This study demonstrates the extended molecular characterization achieved by coupling HPLC with 21T FT-ICR MS for the analysis of wood pyrolysis bio-oils. This approach revealed approximately 3,000 additional monoisotopic O_x molecular formulas compared to direct-infusion MS, offering deeper insights into bio-oil composition, including lignin-derived oligomers and carbohydrate-like species. By improving the detection of species with lower ionization efficiencies, such as carbohydrates and highly aromatic compounds, the method provides a more comprehensive understanding of molecular composition, isomeric diversity, and functional group distribution within bio-oils.

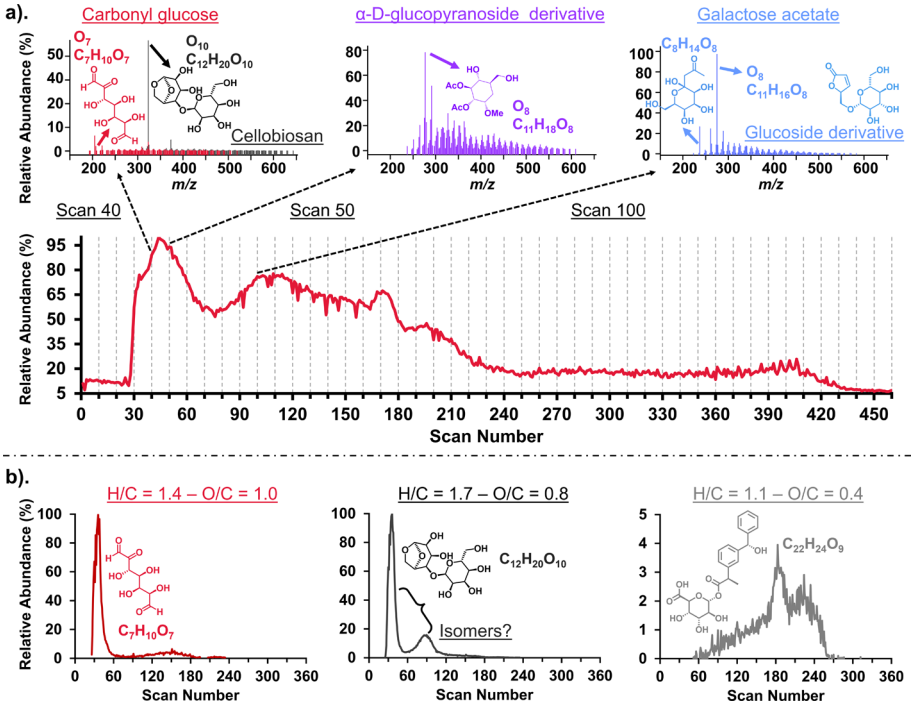

Figure 8. (a) Total ion chromatogram (TIC) for the F4 UASE fraction from the upgraded RTI bio-oil analyzed via HPLC -ESI 21T FT-ICR MS, with extracted mass spectra for selected scans: Scan 40 (O_7 and O_{10} classes), Scan 50 (O_8 class), and Scan 100 (O_8 class). Molecular formulas and potential structures are shown for the most prominent peaks. (b) Single ion chromatograms for selected molecular formulas ($C_7H_{10}O_7$, $C_{12}H_{20}O_{10}$, and $C_{22}H_{24}O_9$), illustrating distinct elution patterns, potential isomers, and the impact of oxygen content and molecular structure on retention behavior. Molecular formulas are reported as neutral compositions.

https://doi.org/10.1021/acs.energyfuels.4c05674
Energy Fuels 2025, 39, 3575−3588

The fractionation of bio-oils, visualized through van Krevelen diagrams, enabled the identification of distinct compositional regions, such as oxygenates in the biomass region and highly aromatic species. The method's ability to detect a broader range of oxygen-containing compounds, including those in the carbohydrate and "highly-aromatic" regions, further highlights its superiority over direct-infusion MS.

A crucial aspect of this approach is the HPLC separation mechanism, which leverages the acidic properties of bio-oil components and their interactions with the basic functionalities of the stationary phase. In the absence of diethylamine (DEA), acidic compounds are strongly retained on the stationary phase, while nonacidic and mildly acidic species elute with methanol. When DEA is introduced, the separation occurs through partition chromatography, allowing the acids to equilibrate between the DEA-containing mobile phase and the stationary phase. Molecules with a higher O/C ratio are retained longer due to stronger hydrogen bonding with the stationary phase, but as the water content in the mobile phase increases, these compounds gradually elute. This process is driven by partitioning behavior, without relying on ionization or pH effects, allowing for efficient elution of oxygen-rich species that are otherwise difficult to separate using conventional reversed-phase chromatography.

Furthermore, HPLC-MS consistently identified more unique molecular species across all bio-oil fractions, including the challenging F4 UASE fraction, where HPLC-MS detected nearly three times the number of unique species compared to direct-infusion MS. This expanded molecular coverage, particularly in oxygen-deficient molecules, aromatic species, and carbohydrates, highlights the method's value in providing deeper insights into the molecular complexity of bio-oils.

This work demonstrates the potential of combining chromatography with ultrahigh-resolution mass spectrometry to enhance molecular-level analysis of complex bio-oils. By identifying previously undetectable molecular species, including recalcitrant aromatic compounds and low-molecular-weight carbohydrates, this approach provides critical insights for optimizing upgrading strategies and developing tailored catalytic solutions. Furthermore, the methodology's adaptability to other complex mixtures, such as emerging contaminants (e.g., water-solubles leached from petroleum-based materials), broadens its applicability beyond bio-oils.

To complement this study, future research could relate biomass feedstock types and pyrolysis conditions to compositional trends in bio-oils, similar to approaches in petroleum geochemistry. Exploring these connections through van Krevelen diagrams and DBE vs carbon number plots may provide valuable insights into the effects of feedstock composition, pyrolysis temperature, and catalyst use. Future efforts will focus on exploring the isomeric diversity of species through MS^n analysis, conducted simultaneously with HPLC FT-ICR MS. This will be facilitated by recent enhancements to the 21T FT-ICR instrument, which is now equipped with an Orbitrap Eclipse Tribrid front-end. Additionally, incorporating cutting-edge technologies such as trapped ion mobility spectrometry (TIMS) will further enhance our ability to investigate isomer distribution.[67] To extend our compositional coverage, APCI and APPI will be employed to explore nonpolar components in bio-oil samples. Preliminary results indicate that bio-oil samples, both before and after advanced catalytic upgrading, contain abundant species with shared molecular formulas and a common compositional range. The overlap observed in van Krevelen diagrams highlights the need for a deeper understanding of these species, including whether they represent recalcitrant compounds (or molecules that remain structurally unchanged during upgrading) or isomers. By resolving isomeric diversity and identifying recalcitrant compounds, we aim to refine upgrading strategies, optimizing bio-oil processing and improving the efficiency of sustainable energy applications.

■ ASSOCIATED CONTENT

Supporting Information

The Supporting Information is available free of charge at https://pubs.acs.org/doi/10.1021/acs.energyfuels.4c05674.

Information about model compounds, and TICs and van Krevelen diagrams for additional bio-oil fractions (PDF)

■ AUTHOR INFORMATION

Corresponding Authors

Martha L. Chacón-Patiño − *National High Magnetic Field Laboratory, Tallahassee, Florida 32310, United States; International Joint Laboratory for Complex Matrices Molecular Characterization, iC2MC, TRTG, Gonfreville 76700 Harfleur, France;* orcid.org/0000-0002-7273-5343; Email: chacon@magnet.fsu.edu

Ryan P. Rodgers − *National High Magnetic Field Laboratory, Tallahassee, Florida 32310, United States; International Joint Laboratory for Complex Matrices Molecular Characterization, iC2MC, TRTG, Gonfreville 76700 Harfleur, France; E2S UPPA, CNRS, IPREM, Universite de Pau et des Pays de l'Adour, 64053 Pau, France; Department of Chemistry and Biochemistry, Florida State University, Tallahassee, Florida 32306, United States;* orcid.org/0000-0003-1302-2850; Email: rodgers@magnet.fsu.edu

Authors

Joseph W. Frye-Jones − *National High Magnetic Field Laboratory, Tallahassee, Florida 32310, United States;* orcid.org/0000-0003-3618-8052

Lissa C. Anderson − *National High Magnetic Field Laboratory, Tallahassee, Florida 32310, United States; Department of Chemistry and Biochemistry, Florida State University, Tallahassee, Florida 32306, United States;* orcid.org/0000-0001-8633-0251

Winston K. Robbins − *National High Magnetic Field Laboratory, Tallahassee, Florida 32310, United States;* orcid.org/0000-0003-3821-1287

Germain Salvato Vallverdu − *International Joint Laboratory for Complex Matrices Molecular Characterization, iC2MC, TRTG, Gonfreville 76700 Harfleur, France; E2S UPPA, CNRS, IPREM, Universite de Pau et des Pays de l'Adour, 64053 Pau, France;* orcid.org/0000-0003-1116-8776

Álvaro J. Tello-Rodríguez − *National High Magnetic Field Laboratory, Tallahassee, Florida 32310, United States*

Wladimir Ruiz − *International Joint Laboratory for Complex Matrices Molecular Characterization, iC2MC, TRTG, Gonfreville 76700 Harfleur, France; E2S UPPA, CNRS, IPREM, Universite de Pau et des Pays de l'Adour, 64053 Pau, France*

German Gascon − *E2S UPPA, CNRS, IPREM, Universite de Pau et des Pays de l'Adour, 64053 Pau, France*

Christopher P. Rüger − *International Joint Laboratory for Complex Matrices Molecular Characterization, iC2MC,*

https://doi.org/10.1021/acs.energyfuels.4c05674
Energy Fuels 2025, 39, 3575−3588

TRTG, Gonfreville 76700 Harfleur, France; Joint Mass Spectrometry Centre, Department of Analytical and Technical Chemistry, University of Rostock, Rostock 18059, Germany; orcid.org/0000-0001-9634-9239

David C. Dayton − *Technology Advancement and Commercialization, RTI International, Research Triangle Park, North Carolina 27709, United States;* orcid.org/0000-0003-3244-3722

Pierre Giusti − *International Joint Laboratory for Complex Matrices Molecular Characterization, iC2MC, TRTG, Gonfreville 76700 Harfleur, France; Total Energies Refining & Chemicals, Total Research & Technology, Gonfreville 76700 Harfleur, France;* orcid.org/0000-0002-9569-3158

Charlotte Mase − *International Joint Laboratory for Complex Matrices Molecular Characterization, iC2MC, TRTG, Gonfreville 76700 Harfleur, France; Total Energies Refining & Chemicals, Total Research & Technology, Gonfreville 76700 Harfleur, France; University of Rouen, Mont-Saint-Aignan 76821, France*

Caroline Barrère-Mangote − *International Joint Laboratory for Complex Matrices Molecular Characterization, iC2MC, TRTG, Gonfreville 76700 Harfleur, France; Total Energies Refining & Chemicals, Total Research & Technology, Gonfreville 76700 Harfleur, France*

Carlos Afonso − *International Joint Laboratory for Complex Matrices Molecular Characterization, iC2MC, TRTG, Gonfreville 76700 Harfleur, France; University of Rouen, Mont-Saint-Aignan 76821, France;* orcid.org/0000-0002-2406-5664

Brice Bouyssiere − *International Joint Laboratory for Complex Matrices Molecular Characterization, iC2MC, TRTG, Gonfreville 76700 Harfleur, France; E2S UPPA, CNRS, IPREM, Universite de Pau et des Pays de l'Adour, 64053 Pau, France;* orcid.org/0000-0001-5878-6067

Complete contact information is available at: https://pubs.acs.org/10.1021/acs.energyfuels.4c05674

Author Contributions

The manuscript was written with contributions from all authors who have approved the final version.

Notes

The authors declare no competing financial interest.

■ ACKNOWLEDGMENTS

Part of this work was performed at The National High Magnetic Field Laboratory (MagLab), funded by the National Science Foundation divisions of materials research and chemistry through DMR-2128556 and the State of Florida.

■ REFERENCES

(1) Struhs, E.; Mirkouei, A.; Ramirez-Corredores, M. M.; McDonald, A. G.; Chacon, M. L. Overview and Technology Opportunities for Thermochemically-Produced Bio-Blendstocks. *Journal of Environmental Chemical Engineering.* **2021**, *9*, No. 106255.

(2) Lam, C. H.; Das, S.; Erickson, N. C.; Hyzer, C. D.; Garedew, M.; Anderson, J. E.; Wallington, T. J.; Tamor, M. A.; Jackson, J. E.; Saffron, C. M. Towards Sustainable Hydrocarbon Fuels with Biomass Fast Pyrolysis Oil and Electrocatalytic Upgrading. *Sustain Energy Fuels* **2017**, *1* (2), 258−266.

(3) Wang, K.; Dayton, D. C.; Peters, J. E.; Mante, O. D. Reactive Catalytic Fast Pyrolysis of Biomass to Produce High-Quality Bio-Crude. *Green Chem.* **2017**, *19* (14), 3243−3251.

(4) Dayton, D. C.; Mante, O. D.; Weiner, J. Effect of Temperature on the Pilot-Scale Catalytic Pyrolysis of Loblolly Pine. *Energy Fuels* **2021**, *35* (16), 13181−13190.

(5) Chen, X.; Che, Q.; Li, S.; Liu, Z.; Yang, H.; Chen, Y.; Wang, X.; Shao, J.; Chen, H. Recent Developments in Lignocellulosic Biomass Catalytic Fast Pyrolysis: Strategies for the Optimization of Bio-Oil Quality and Yield. *Fuel Process. Technol.* **2019**, *196*, No. 106180.

(6) Chireshe, F.; Collard, F. X.; Görgens, J. F. Production of Low Oxygen Bio-Oil via Catalytic Pyrolysis of Forest Residues in a Kilogram-Scale Rotary Kiln Reactor. *J. Cleaner Prod.* **2020**, *260*, No. 120987.

(7) Dayton, D. C.; Wang, K.; Peters, J. E.; Mante, O. D. CHAPTER 5 Catalytic Biomass Pyrolysis with Reactive Gases. In *Fast Pyrolysis of Biomass: Advances in Science and Technology*, 2017; Vol. *1*, pp 78−95.

(8) Veses, A.; López, J. M.; García, T.; Callén, M. S. Prediction of Elemental Composition, Water Content and Heating Value of Upgraded Biofuel from the Catalytic Cracking of Pyrolysis Bio-Oil Vapors by Infrared Spectroscopy and Partial Least Square Regression Models. *J. Anal Appl. Pyrolysis* **2018**, *132*, 102−110.

(9) Mettler, M. S.; Paulsen, A. D.; Vlachos, D. G.; Dauenhauer, P. J. Pyrolytic Conversion of Cellulose to Fuels: Levoglucosan Deoxygenation via Elimination and Cyclization within Molten Biomass. *Energy Environ. Sci.* **2012**, *5* (7), 7864−7868.

(10) Zadeh, Z. E.; Abdulkhani, A.; Aboelazayem, O.; Saha, B. Recent Insights into Lignocellulosic Biomass Pyrolysis: A Critical Review on Pretreatment, Characterization, and Products Upgrading. *Processes* **2020**, *8*, 799.

(11) Fardhyanti, D. S.; Megawati; Chafidz, A.; Prasetiawan, H.; Raharjo, P. T.; Habibah, U.; Abasaeed, A. E. Production of Bio-Oil from Sugarcane Bagasse by Fast Pyrolysis and Removal of Phenolic Compounds. *Biomass Convers Biorefin* **2024**, *14* (1), 217−227.

(12) Ferrell, J. R.; Olarte, M. V.; Christensen, E. D.; Padmaperuma, A. B.; Connatser, R. M.; Stankovikj, F.; Meier, D.; Paasikallio, V. Standardization of Chemical Analytical Techniques for Pyrolysis Bio-Oil: History, Challenges, and Current Status of Methods. *Biofuels, Bioproducts and Biorefining* **2016**, *10* (5), 496−507.

(13) Choi, Y. S.; Johnston, P. A.; Brown, R. C.; Shanks, B. H.; Lee, K. H. Detailed Characterization of Red Oak-Derived Pyrolysis Oil: Integrated Use of GC, HPLC, IC, GPC and Karl-Fischer. *J. Anal Appl. Pyrolysis* **2014**, *110* (1), 147−154.

(14) David, K.; Kosa, M.; Williams, A.; Mayor, R.; Realff, M.; Muzzy, J.; Ragauskas, A. 31P-NMR Analysis of Bio-Oils Obtained from the Pyrolysis of Biomass. *Biofuels* **2010**, *1* (6), 839−845.

(15) Tessarolo, N. S.; Silva, R. C.; Vanini, G.; Pinho, A.; Romão, W.; de Castro, E. V. R.; Azevedo, D. A. Assessing the Chemical Composition of Bio-Oils Using FT-ICR Mass Spectrometry and Comprehensive Two-Dimensional Gas Chromatography with Time-of-Flight Mass Spectrometry. *Microchemical Journal* **2014**, *117*, 68−76.

(16) Cardoso, C. A. L.; Machado, M. E.; Caramão, E. B. Characterization of Bio-Oils Obtained from Pyrolysis of Bocaiuva Residues. *Renew Energy* **2016**, *91*, 21−31.

(17) Ateş, F.; Işikdağ, M. A. Evaluation of the Role of the Pyrolysis Temperature in Straw Biomass Samples and Characterization of the Oils by GC/MS. *Energy Fuels* **2008**, *22* (3), 1936−1943.

(18) Sipilä, K.; Kuoppala, E.; Fagernäs, L.; Oasmaa, A. Characterization of Biomass-Based Flash Pyrolysis Oils. *Biomass Bioenergy* **1998**, *14* (2), 103−113.

(19) Serras-Malillos, A.; Perez-Martinez, B. B.; Iriondo, A.; Acha, E.; Lopez-Urionabarrenechea, A.; Caballero, B. M. Quantification of the Composition of Pyrolysis Oils of Complex Plastic Waste by Gas Chromatography Coupled with Mass Spectrometer Detector. *RSC Adv.* **2024**, *14* (14), 9892−9911.

(20) Lyu, G.; Wu, S.; Zhang, H. Estimation and Comparison of Bio-Oil Components from Different Pyrolysis Conditions. *Front. Energy Res.* **2015**, *3*, 28.

(21) Vilas-Boas, A. C. M.; Tarelho, L. A. C.; Moura, J. M. O.; Gomes, H. G. M. F.; Marques, C. C.; Pio, D. T.; Nunes, M. I. S.; Silvestre, A. J. D. Methodologies for Bio-Oil Characterization from Biomass Pyrolysis: A

Review Focused on GC-MS. *Journal of Analytical and Applied Pyrolysis.* **2025**, *185*, No. 106850.
(22) Marshall, A. G.; Rodgers, R. P. Petroleomics: Chemistry of the Underworld. *Proc. Natl. Acad. Sci. U. S. A.* **2008**, *105* (47), 18090−18095.
(23) Islam, A.; Cho, Y.; Ahmed, A.; Kim, S. Data Interpretation Methods for Petroleomics. *Mass Spectrometry Letters* **2012**, *3* (3), 63−67.
(24) Chacon-Patino, M. L.; Rodgers, R. P.; Frye-Jones, J.; Anderson, L.; Giusti, P. Novel LC Separation for Comprehensive Analysis of Net-Zero Bio-Oils by Ultra-High-Resolution Mass Spectrometry. In *72 rd Conference on Mass Spectrometry and Allied Topics*; Anaheim, CA, 2024.
(25) Mase, C.; Hubert-Roux, M.; Afonso, C.; Giusti, P. Contribution of Atmospheric Pressure Chemical Ionization Mass Spectrometry for the Characterization of Bio-Oils from Lignocellulosic Biomass: Comparison with Electrospray Ionization and Atmospheric Pressure Photoionization. *J. Anal Appl. Pyrolysis* **2022**, *167*, No. 105694.
(26) Ware, R. L.; Rowland, S. M.; Rodgers, R. P.; Marshall, A. G. Advanced Chemical Characterization of Pyrolysis Oils from Landfill Waste, Recycled Plastics, and Forestry Residue. *Energy Fuels* **2017**, *31* (8), 8210−8216.
(27) Palacio Lozano, D. C.; Jones, H. E.; Barrow, M. P.; Wills, M. Chemoselective Derivatisation and Ultrahigh Resolution Mass Spectrometry for the Determination of Hydroxyl Functional Groups within Complex Bio-Oils. *RSC Adv.* **2023**, *13* (26), 17727−17741.
(28) Chacón-Patiño, M. L.; Mase, C.; Maillard, J. F.; Barrère-Mangote, C.; Dayton, D. C.; Afonso, C.; Giusti, P.; Rodgers, R. P. Petroleomics Approach to Investigate the Composition of Upgrading Products from Pyrolysis Bio-Oils as Determined by High-Field FT-ICR MS. *Energy Fuels* **2023**, *37* (21), 16612−16628.
(29) Jarvis, J. M.; Page-Dumroese, D. S.; Anderson, N. M.; Corilo, Y.; Rodgers, R. P. Characterization of Fast Pyrolysis Products Generated from Several Western USA Woody Species. *Energy Fuels* **2014**, *28* (10), 6438−6446.
(30) Ware, R. L. L.; Rodgers, R. P.; Marshall, A. G.; Mante, O. D.; Dayton, D. C.; Verdier, S.; Gabrielsen, J.; Rowland, S. M. Detailed Chemical Composition of an Oak Biocrude and Its Hydrotreated Product Determined by Positive Atmospheric Pressure Photoionization Fourier Transform Ion Cyclotron Resonance Mass Spectrometry. *Sustain Energy Fuels* **2020**, *4* (5), 2404−2410.
(31) Palacio Lozano, D. C.; Jones, H. E.; Ramirez Reina, T.; Volpe, R.; Barrow, M. P. Unlocking the Potential of Biofuels: Via Reaction Pathways in van Krevelen Diagrams. *Green Chem.* **2021**, *23* (22), 8949−8963.
(32) Palacio Lozano, D. C.; Lester, D. W.; Town, J. S.; McKenna, A. M.; Wills, M. Assessment of Accelerated Aging Effect of Bio-Oil Fractions Utilizing Ultrahigh-Resolution Mass Spectrometry and k-Means Clustering of van Krevelen Compositional Space. *Energy Fuels* **2024**, *38* (17), 16473−16489.
(33) Chacón-Patiño, M. L.; Rowland, S. M.; Rodgers, R. P. Advances in Asphaltene Petroleomics. Part 1: Asphaltenes Are Composed of Abundant Island and Archipelago Structural Motifs. *Energy Fuels* **2017**, *31* (12), 13509−13518.
(34) Lazzari, E.; Arena, K.; Caramão, E. B.; Herrero, M. Quantitative Analysis of Aqueous Phases of Bio-Oils Resulting from Pyrolysis of Different Biomasses by Two-Dimensional Comprehensive Liquid Chromatography. *J. Chromatogr A* **2019**, *1602*, 359−367.
(35) Crepier, J.; Le Masle, A.; Charon, N.; Albrieux, F.; Heinisch, S. Development of a Supercritical Fluid Chromatography Method with Ultraviolet and Mass Spectrometry Detection for the Characterization of Biomass Fast Pyrolysis Bio Oils. *J. Chromatogr A* **2017**, *1510*, 73−81.
(36) Rowland, S.; Smith, D.; Blakney, G.; Hendrickson, C.; Rodgers, R. Online Coupling of Liquid Chromatography with Fourier Transform Ion Cyclotron Resonance Mass Spectrometry at 21 T Provides Fast and Unique Insight into Crude Oil Composition. *Anal. Chem.* **2021**, *93*, 13749−13754.
(37) Ruiz, W.; Gascon, G.; Chacón-Patiño, M. L.; Rodgers, R. P.; Dayton, D. C.; Barrère-Mangote, C.; Giusti, P.; Bouyssiere, B. Ultrasound-Assisted Sequential Extraction for Lignocellulose Pyrolysis Bio-Oil Fractionation. Part I: Method Development. *Energy Fuels* **2024**, *38*, 17687.
(38) Smith, D. F.; Podgorski, D. C.; Rowland, S. M.; Hendrickson, C. L. 21 T FT-ICR Mass Spectrometer for Complex Mixture Analysis. In *Proceedings of the ASMS Asilomar Conference 2016 Pacific Grove*, CA, USA, October 14−18, 2016.
(39) Kaiser, N. K.; Savory, J. J.; Hendrickson, C. L. Controlled Ion Ejection from an External Trap for Extended m/z Range in FT-ICR Mass Spectrometry. *J. Am. Soc. Mass Spectrom.* **2014**, *25* (6), 943−949.
(40) Nikolaev, E. N.; Boldin, I. A.; Jertz, R.; Baykut, G. Initial Experimental Characterization of a New Ultra-High Resolution FTICR Cell with Dynamic Harmonization. *J. Am. Soc. Mass Spectrom.* **2011**, *22* (7), 1125−1133.
(41) Smith, D. F.; Podgorski, D. C.; Rodgers, R. P.; Blakney, G. T.; Hendrickson, C. L. 21 T FT-ICR Mass Spectrometer for Ultrahigh-Resolution Analysis of Complex Organic Mixtures. *Anal. Chem.* **2018**, *90* (3), 2041−2047.
(42) Blakney, G. T.; Hendrickson, C. L.; Marshall, A. G. Predator Data Station: A Fast Data Acquisition System for Advanced FT-ICR MS Experiments. *Int. J. Mass Spectrom.* **2011**, *306* (2−3), 246−252.
(43) Sueur, M.; Maillard, J. F.; Lacroix-Andrivet, O.; Rüger, C. P.; Giusti, P.; Lavanant, H.; Afonso, C. PyC2MC: An Open-Source Software Solution for Visualization and Treatment of High-Resolution Mass Spectrometry Data. *J. Am. Soc. Mass Spectrom.* **2023**, *34* (4), 617−626.
(44) Chacón-Patinõ, M. L.; Smith, D. F.; Hendrickson, C. L.; Marshall, A. G.; Rodgers, R. P. Advances in Asphaltene Petroleomics. Part 4. Compositional Trends of Solubility Subfractions Reveal That Polyfunctional Oxygen-Containing Compounds Drive Asphaltene Chemistry. *Energy Fuels* **2020**, *34*, 3013−3030.
(45) Louwes, A. C.; Basile, L.; Yukananto, R.; Bhagwandas, J. C.; Bramer, E. A.; Brem, G. Torrefied Biomass as Feed for Fast Pyrolysis: An Experimental Study and Chain Analysis. *Biomass Bioenergy* **2017**, *105*, 116−126.
(46) Ahmad, M.; Subawi, H. New Van Krevelen Diagram and Its Correlation with the Heating Value of Biomass. *Res. J. Agric. Environ. Manage.* **2013**, *2* (10), 295−301.
(47) Al Jamri, M.; Li, J.; Smith, R. Molecular Characterisation of Biomass Pyrolysis Oil and Petroleum Fraction Blends. *Comput. Chem. Eng.* **2020**, *140*, No. 106906.
(48) Chen, H.; Xu, H.; Zhu, H.; Yan, S.; Zhang, S.; Zhang, H.; Guo, X.; Hu, X.; Gao, W. A Review on Bioslurry Fuels Derived from Bio-Oil and Biochar: Preparation, Fuel Properties and Application. *Fuel.* **2024**, *355*, No. 129283.
(49) Maneechakr, P.; Karnjanakom, S. Improving the Bio-Oil Quality via Effective Pyrolysis/Deoxygenation of Palm Kernel Cake over a Metal (Cu, Ni, or Fe)-Doped Carbon Catalyst. *ACS Omega* **2021**, *6* (30), 20006−20014.
(50) McKenna, A. M.; Chacón-Patiño, M. L.; Chen, H.; Blakney, G. T.; Mentink-Vigier, F.; Young, R. B.; Ippolito, J. A.; Borch, T. Expanding the Analytical Window for Biochar Speciation: Molecular Comparison of Solvent Extraction and Water-Soluble Fractions of Biochar by FT-ICR Mass Spectrometry. *Anal. Chem.* **2021**, *93* (46), 15365−15372.
(51) Rodgers, R. P.; Mapolelo, M. M.; Robbins, W. K.; Chacón-Patiño, M. L.; Putman, J. C.; Niles, S. F.; Rowland, S. M.; Marshall, A. G. Combating Selective Ionization in the High Resolution Mass Spectral Characterization of Complex Mixtures. *Faraday Discuss.* **2019**, *218*, 29.
(52) Rowland, S. M.; Robbins, W. K.; Corilo, Y. E.; Marshall, A. G.; Rodgers, R. P. Solid-Phase Extraction Fractionation To Extend the Characterization of Naphthenic Acids in Crude Oil by Electrospray Ionization Fourier Transform Ion Cyclotron Resonance Mass Spectrometry. *Energy Fuels* **2014**, *28*, 5043−5048.
(53) Frye-Jones, J. W.; Chacón-Patiño, M. L.; Marshall, A. G.; Rodgers, R. P. Photoinduced Oxidation and Polymerization in Oil-Soluble Products and Interfacial Material from Petroleum Weathering. *Energy Fuels* **2025**, *39*, 1031.
(54) Boreen, A. L.; Edhlund, B. L.; Cotner, J. B.; Mcneill, K. Indirect Photodegradation of Dissolved Free Amino Acids: The Contribution of

https://doi.org/10.1021/acs.energyfuels.4c05674
Energy Fuels 2025, 39, 3575−3588

Singlet Oxygen and the Differential Reactivity of DOM from Various Sources. *Environ. Sci. Technol.* **2008**, *42* (15), 5492−5498.
(55) Rodgers, R. P.; Rodgers, R. P.; Robbins, W.; Giraldo, D.; Frye-Jones, J.; Weisbord, C.; Marshall, A. G.; Bouyssiere, B.; Giusti, P. Online LC/21T FT-ICR MS and ICP-MS Analysis of Dissolved Organic Matter (DOM). In *71st Conference on Mass Spectrometry and Allied Topics*; Houston, TX, 2023.
(56) Frye-Jones, J. W.; Chacon-Patino, M. L.; Anderson, L. C.; Tello-Rodriguez, A. J.; Robbins, W. K.; Marshall, A. G.; Rodgers, R. P. Expanding Molecular Compositional Coverage of Water-Soluble Emerging Contaminants with Liquid Chromatography−Ultrahigh-Resolution Mass Spectrometry. In *72nd Conference on Mass Spectrometry and Allied Topics*; ASMS: Anaheim, CA, 2024.
(57) Glenne, E.; Samuelsson, J.; Leek, H.; Forssén, P.; Klarqvist, M.; Fornstedt, T. Systematic Investigations of Peak Distortions Due to Additives in Supercritical Fluid Chromatography. *J. Chromatogr. A* **2020**, *1621*, No. 461048.
(58) Gasco-Lopez, A. I.; Santos-Montes, A.; Izquierdo-Hornillos, R. *The Effect of Different Amines Added to Eluents as Silanol Masking Agents on the Chromatographic Behavior of Some Diuretics in Reversed-Phase High-Performance Liquid Chromatography Using C 18 Packings*, 1997; Vol. *35*. https://academic.oup.com/chromsci/article/35/11/525/272680.
(59) Binh, V. N.; Hue, V. T. P.; Ha, P. T. T. Peak Shape Enhancement Using Diethylamine in Hydrophilic Liquid Interaction Chromatography: Application in Simultaneous Determination of Methionine and Paracetamol. *J. Pharm. Biomed. Anal.* **2021**, *203*, No. 114214.
(60) Ruiz, W.; Gascon, G.; Rodgers, R. P.; Dayton, D. C.; Barrère-Mangote, C.; Giusti, P.; Bouyssiere, B.; Chacón-Patiño, M. L. Ultrasound-Assisted Sequential Extraction for Lignocellulose Pyrolysis Bio-Oil Fractionation. Part II: Comparative Application. *Energy Fuels* **2024**, *38* (18), 17697−17705.
(61) Xiong, Z.; Syed-Hassan, S. S. A.; Xu, J.; Wang, Y.; Hu, S.; Su, S.; Zhang, S.; Xiang, J. Evolution of Coke Structures during the Pyrolysis of Bio-Oil at Various Temperatures and Heating Rates. *J. Anal Appl. Pyrolysis* **2018**, *134*, 336−342.
(62) Zhou, X.; Nolte, M. W.; Mayes, H. B.; Shanks, B. H.; Broadbelt, L. J. Experimental and Mechanistic Modeling of Fast Pyrolysis of Neat Glucose-Based Carbohydrates. 1. Experiments and Development of a Detailed Mechanistic Model. *Ind. Eng. Chem. Res.* **2014**, *53* (34), 13274−13289.
(63) Lazzari, E.; Mase, C.; Dayton, D. C.; Marceau, S.; Purcaro, G.; Focant, J. F.; Piparo, M.; Giusti, P. Exploring Molecular Composition of Upgraded Pyrolysis Bio-Oil Using GC × GC-(EI/PI)-TOF MS with Different Column Set-Ups. *J. Anal. Appl. Pyrolysis* **2024**, *181*, No. 106569.
(64) Mase, C.; Moulian, R.; Lazzari, E.; Garnier, C.; Piparo, M.; Hubert-Roux, M.; Afonso, C.; Dayton, D. C.; Barrère-Mangote, C.; Giusti, P. Comparison of Lignocellulosic-Based Biomass Pyrolysis Processes by Multi-Scale Molecular Characterization. *J. Anal. Appl. Pyrolysis* **2024**, *177*, No. 106354.
(65) Liaw, S. S.; Haber Perez, V.; Zhou, S.; Rodriguez-Justo, O.; Garcia-Perez, M. Py-GC/MS Studies and Principal Component Analysis to Evaluate the Impact of Feedstock and Temperature on the Distribution of Products during Fast Pyrolysis. *J. Anal Appl. Pyrolysis* **2014**, *109*, 140−151.
(66) Wang, H.; Wang, Y.; Sun, X.; Hu, H.; Peng, Q. Two Functional Post-Cross-Linked Polystyrene Resins: Effect of Structure on the Enhanced Removal of Benzene Sulfonic Acid. *Colloids Surf., A* **2020**, *588*, No. 124398.
(67) Wootton, C. A.; Maillard, J.; Theisen, A.; Brabeck, G. F.; Schat, C. L.; Rüger, C. P.; Afonso, C.; Giusti, P. A Gated TIMS FTICR MS Instrument to Decipher Isomeric Content of Complex Organic Mixtures. *Anal. Chem.* **2024**, *96* (28), 11343−11352.

https://doi.org/10.1021/acs.energyfuels.4c05674
Energy Fuels 2025, 39, 3575−3588